Kuwait J. Sci. **45 (4)** pp 37 - 45, 2018

Femtosecond laser based deposition of nanoparticles on a thin film and its characterization

Jahja Kokaj[1,*], Ali Shuaib[2], Yacoub Makdisi[1], Remya Nair[1] and Joseph Mathew[1]

[1]*Dept. of Physics, Faculty of Science, Kuwait University, P.O. Box 5969, 13060 Safat, Kuwait*

[2]*Biomedical Eng. Unit, Physiology Dept., Faculty of Medicine, Kuwait University*

**Corresponding author: jkokaj@yahoo.com*

Abstract

Femtosecond laser based deposition of nanoparticles is a promising technique for the formation of homogenous thin films. The introduction provides a literature review related to the techniques for thin film deposition including pulsed-laser deposition (PLD). We then describe the homemade chamber used for PLD with a femtosecond laser. An atomic force microscope (AFM) was used to measure the characteristics of the obtained films. Thickness, roughness and texture of the surface of the films were visualized using this technique. X-ray diffraction and scanning electron microscopy were used to characterize the obtained thin layer of nanoparticle film. The band gap energy of zinc oxide film was determined using UV-VIS characterization,

Keywords: Ablation; characterization; deposition; femtosecond laser; nanoparticles.

1. Introduction

The use of laser for transferring particles from a metal to a substrate was first reported in the 1960s (Smith & Turner, 1965; Helmut & Tourtellotte, 1969). However, cheaper and simpler techniques have also been used to deposit thin films onto a substrate. Chemical deposition is a robust, economical and useful technique (Kokaj & Rakhshani 2004; Rakhshani *et al.* 2007; Rakhshani *et al.* 2007; Rakhshani *et al.* 2009; Jahja 2011). Vapor and chemical deposition techniques are versatile as well (Tan *et al.,* 2005; Jayadev *et al.*, 2009). Detailed models and approaches for characterizing film deposition have been discussed in the literature. (Metev & Veiko, 1998; Adel *et al.*, 2013; Christian, 2012; Willmott & Huber, 2000; Sivanandan *et al.*, 2014). Chrisey & Hubler (1994), Lowndes *et al.* (1996), Willmott & Huber (2000), and Willmott (2004) present versatile and relevant procedures for PLD.

The Pulsed Electron Deposition technique allows for useful experimental approaches for the development of PLD. This technique has been compared with other techniques by several authors (Jiang & Xu, 1989; Scholch *et al.*, 1989; Höbel *et al.*, 1990; Harshavardhan & Strikovski, 2005; Christen *et al.*, 2005).

Schlom *et al.* (2001) and Warusawithana *et al.* (2003) showed that PLD can be a complementary technique to the molecular-beam epitaxial method. Lee *et al.* (2005) and Yamada *et al. (*2002*)* have shown that complex materials can be used for the growth of useful films with smooth surfaces. Geohegan (1994), Geohegan & Puretzky (1996), and Sambri *et al.* (2007) explained the characterization and diagnostics of PD films and how they play an important role in the deposition of high quality films which are useful for electronic and possible photovoltaic sources.

Characterization of the nanoscopic deposited structures, atomic growth and desired smoothness of the surface films can be performed using SEM, AFM and XRD techniques. The deposited film with the desired parameters can be used in electronics as photovoltaic energy sources and spatial light modulators. The thickness, surface structure, and chemical content can be measured using SEM technique. UV-VIS characterization can be used to measure and determine the nanoscopic and microscopic properties of the film. Quantum well can be a relevant parameter for the possible use of the film as a photovoltaic source or electronic device. Thus it can be studied using this technique.

A homemade chamber was used in this study for PLD of the nanostructures. Its description and functionality at elevated temperature and low pressure is given. Figure 1 shows the mechanism for film deposition mediated by femtosecond laser pulses and plasma formed after the extraction of atoms, materials from the target. The characterization of the obtained films is presented after a description of the experimental procedure. The results obtained from AFM, SEM, XRD and UV-VIS are shown.

2. Ablation and deposition

Femtosecond laser pulsed light was focused—on the target material zinc oxide (ZnO) (Product No. 752681, Sigma Aldrich). It was targeted where it evaporates its surface, creating a plasma plume. The plume results from

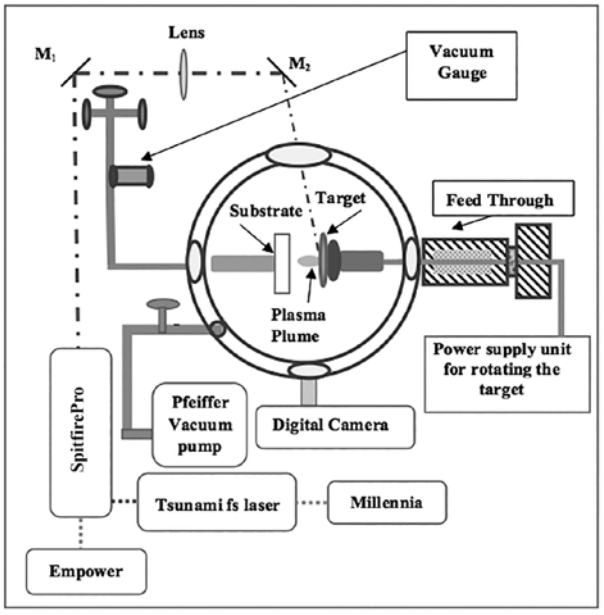

Fig. 1. Experimental setup for Pulsed Laser Deposition

condensation of the material vapor on a substrate placed in the vicinity of the target surface. From the vaporized target, nanoparticles were scattered, reaching a surface substrate placed in front of the target (Figure 1). The target to substrate distance varied from 10 mm to 60 mm. The best distance for coating was found to be 20 mm. The target distanced remained constant throughout the experiment, and the target was kept unbiased.The adhesion of particles on the surface of the substrate constitutes deposition of a thin film. A homemade cylindrical chamber (Figure 2a) was used for Pulsed Laser Deposition (PLD). This is a stainless steel oven with 5 openings, one of which is for vacuum connections. Another opening is for electrical connections to the motor that rotates the target holder. The other three openings are closed with BK7 windows. The topmost window is used to focus the laser beam onto the target holder. The internal parts of the PLD chamber can be seen in Figure 2b. The target is placed on the rotating plate. In its vicinity is a parallel plate on which the glass substrate is placed.

The pulsed laser deposition was performed in a vacuum environment of the order 10^{-3} mbar residual pressure. The PLD chamber was connected to a vacuum system comprised of a Pfeiffer vacuum pump, HiCube (Model: TC 110) with a MKS vacuum display and a Micropirani Baratron pressure sensor.

3. Visualization of the mechanism of the film deposition. Ablation mediated by plasma plume and deposition of the particles on the substrate

The plasma plume generated by the femtosecond amplifier was visualized using a digital camera (Canon IXUS 900 Ti). Images are shown in Figure 3b. The plume was created by an ultrafast femtosecond laser light with a wavelength 797 nm. Figure 3(b) shows a dense thick white plume expanding from the core (target surface) which propagates towards the substrate. Nucleation starts on its surface. During this process, the plume expands from the target, which is a vapor, and recompenses onto the glass substrate. The expanding plume mainly consists of electrons, ions and neutral atoms extracted from the target. The main mechanism behind femtosecond ablation is the coulomb explosion, in which the atoms are highly ionized. Here an electric field is created between the separated charges or highly ionized target atoms formed between the target surface and ejected electrons. The schematics of the plasma plume development on the target surface are shown in Figure3a. The plasma plume generated by laser was recorded using a digital camera. Its image is shown in Figure 3b. The plume, as shown in the Figure 3b, has a thick white color in the center and a light blue background. The laser-based plasma plume (LPP) from a femtosecond laser has a cylindrical shape. The expanded plume is, therefore, also cylindrical.

The strongest emission seems to be from the portion closest to the target surface. This is the hottest part of the plasma. In a femtosecond laser produced plasma, excited neutrals dominate over ions, which are dominant in

(a) (b)

Fig. 2. (a) chamber used for PLD (b) inside view, target and substrate

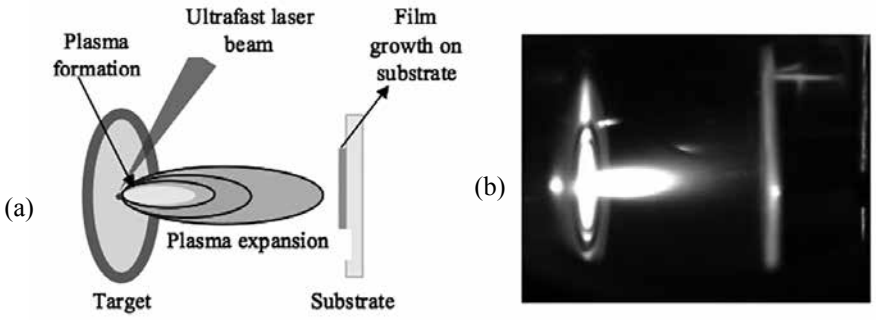

Fig. 3. (a) Schematic of the plasma plume generation, (b) Experimental plasma formation

nanosecond LPP. The plasma produced from a femtosecond laser is short lived because the pulse duration is short. Our experiments for PLD are performed in a vacuum environment of 4×10^{-3} mbar, so the plasma plume was confined to a larger area when compared to the volume size of a plasma generated at standard atmospheric pressure. At higher or atmospheric pressure, the plume was concentrated in a particularly small area. The laser produced plasma from a femtosecond laser propagates in a narrow angular distribution as compared to those produced by a nanosecond laser.

4. Experimental procedure

The target surface was irradiated with a femtosecond laser amplifier (Model: SpitfirePro). An incident light of wavelength of 797 nm and an average power of 3 W were applied to the target. The pulse width of the laser was 117 fs with a repetition rate of 1 kHz. The laser radiation was applied on the target surface continuously for up to 10 minutes. The energy per pulse was 3 mJ. The beam diameter of the laser was 8 mm and was focused onto the target surface for maximum fluence using an IR coated Achromatic Plano convex quartz lens that had a focal length 40 cm. The focused laser beam was irradiated to the target surface through a window placed above the PLD chamber. The generated plasma plume was visualized through the side window and recorded using a CCD camera.

The wavelength and fluency of the laser beam was kept the same throughout the experiment and the only changing parameter was the exposure time of the laser beam onto the target surface. The exposure time varied from 5-10 minutes, and the changes in the obtained film were studied.

Before the process of deposition takes place, the substrate surface should be clean enough to obtain a strong adhesion, otherwise the coating will be easily removed after performing the experiment. Therefore, the glass slide was washed thoroughly with ethanol in an ultrasonic bath for 5 minutes and placed into the chamber (Figure 2b). The chamber was then evacuated up to 4×10^{-3} mbar pressure and the target surface was illuminated with the aligned laser beam. The laser light exposure was controlled by a timer.

The plasma plume was condensed onto the glass slide. After irradiation, the chamber was allowed to fill with air until it reached atmospheric pressure, allowing the chamber top cover to be easily opened so that the substrate could be taken out. The substrate's thin film was cleaned again in an ultrasonic bath to check that the desired adhesion had been achieved. The film was then characterized.

5. Characterization of the thin film

The obtained film was characterized using an electron microscope, nanoscope, X-ray diffraction and other modern techniques. The surface of the film and its macro and micro structure were analyzed.

5.1. Atomic Force Microscopy (AFM)

Atomic Force Microscopy, or nanoscopy, was used mainly to visualize the surface topography of a specimen. It gives information about the surface of a specimen including the roughness and thickness of a coating. The surface topography images obtained by AFM are very clear, allowing details or texture to be seen. Agilent AFM 5420 is used for the characterization of the film. The sample surface topography images can be recorded in different AFM operation modes. The tip and cantilever are driven in a vertical oscillatory motion close to the resonance frequency of the cantilever. As the probe tip approaches the sample surface, the phase and amplitude of the cantilever oscillation are slightly changed due to the tip-sample interaction.

In this operation mode, almost no damage is inflicted to the sample surface because it is nearly contact free. The third case is the intermittent contact mode. This was used for topography measurements. In this intermittent contact mode, the probe tip is not continuously in contact with the sample surface during scanning. Instead the probe sometimes touches the surface, without damaging it. The interaction forces are measured throughout the experiment.

From the analysis of the films using AFM it was found that the films were very rough in nature. Two types of films presented in Figure 4 and Figure 5 were obtained, one with laser exposure time of 10 minutes and the other with 5 minutes. The thickness and roughness measurements of both were made and compared. The results are shown in Table 1.

Table 1. Thickness and roughness of thin film measurements using AFM.

Laser exposure time (min)	Thickness of the film (nm)	Roughnessof the film (nm)
10	866	72
5	537	87.9

The quantitative results in Table 1 show that the thicker film can performed while its roughness decreases. In conclusion, the thicker film, which can be used as a component for spatial light modulation, will also have a smoother surface.

The roughness of the plain substrate was measured using AFM and found to be 3.38 nm RMS in height.

5.2. Scanning Electron Microscopy (SEM)

The surfaces of the ZnO thin film were analyzed with SEM (JEOL's JSM-6300). The Energy Dispersive Spectroscopy (EDS) on SEM allows for the identification of the specific elements present in their relative proportions (in atomic %). It is based on the interaction of incident electrons with material inducing of X-ray excitation from the sample. The characteristic rays are emitted due to the higher energy of an incident electron beam.

The characteristic X-ray spectra identify the chemical content or presence of particular elements in the sample.

Images with a higher resolution were obtained due to shorter wavelength of incident electrons introduced to the film. Figures 6 and 7 show these images for the two types of film. Also shown are the graphs and numerical data that were measured using characteristic X-ray spectra. The numerical data of spectra acquisition and EDS analysis are shown in Figures 6e and 7e.

While the SEM images shown in Figure 6 represent the film deposited by PLD for the time span of 6 min, the

Table 2. Elemental composition of thin film recorded for 10 minutes (obtained from EDS analysis).

Element	Series	unn. C [wt. - %]	norm. C [wt. - %]	Atom. C [at. - %]
Zinc	K series	41.07	50.22	19.80
Oxygen	K series	40.72	49.78	80.20
Total = 81.8 %				

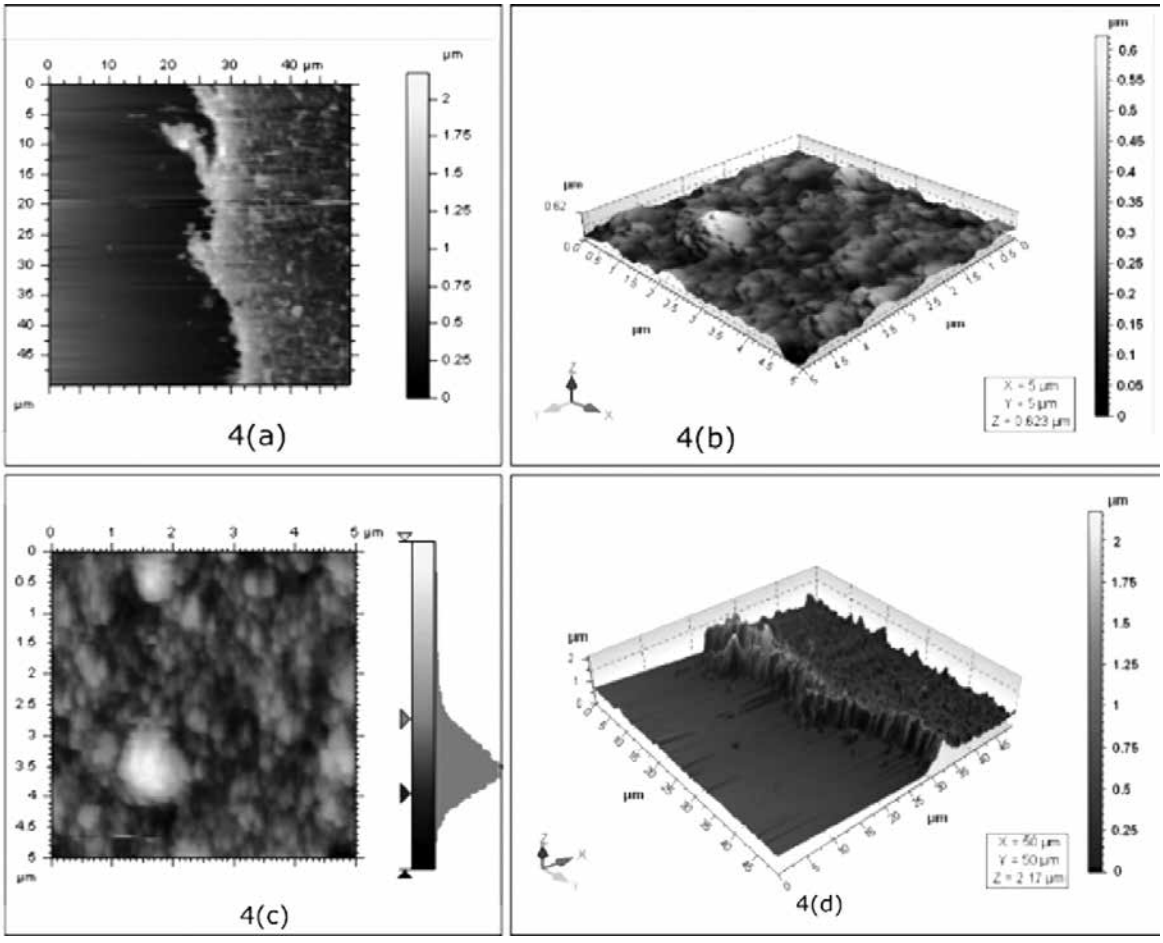

Fig. 4. AFM surface images of ZnO thin films formed on glass substrate with laser exposure (T= 10 min) (a) thickness measurement (b) 3-D view of film (c) roughness measurement of film, and (d) roughness measurement 3-D view

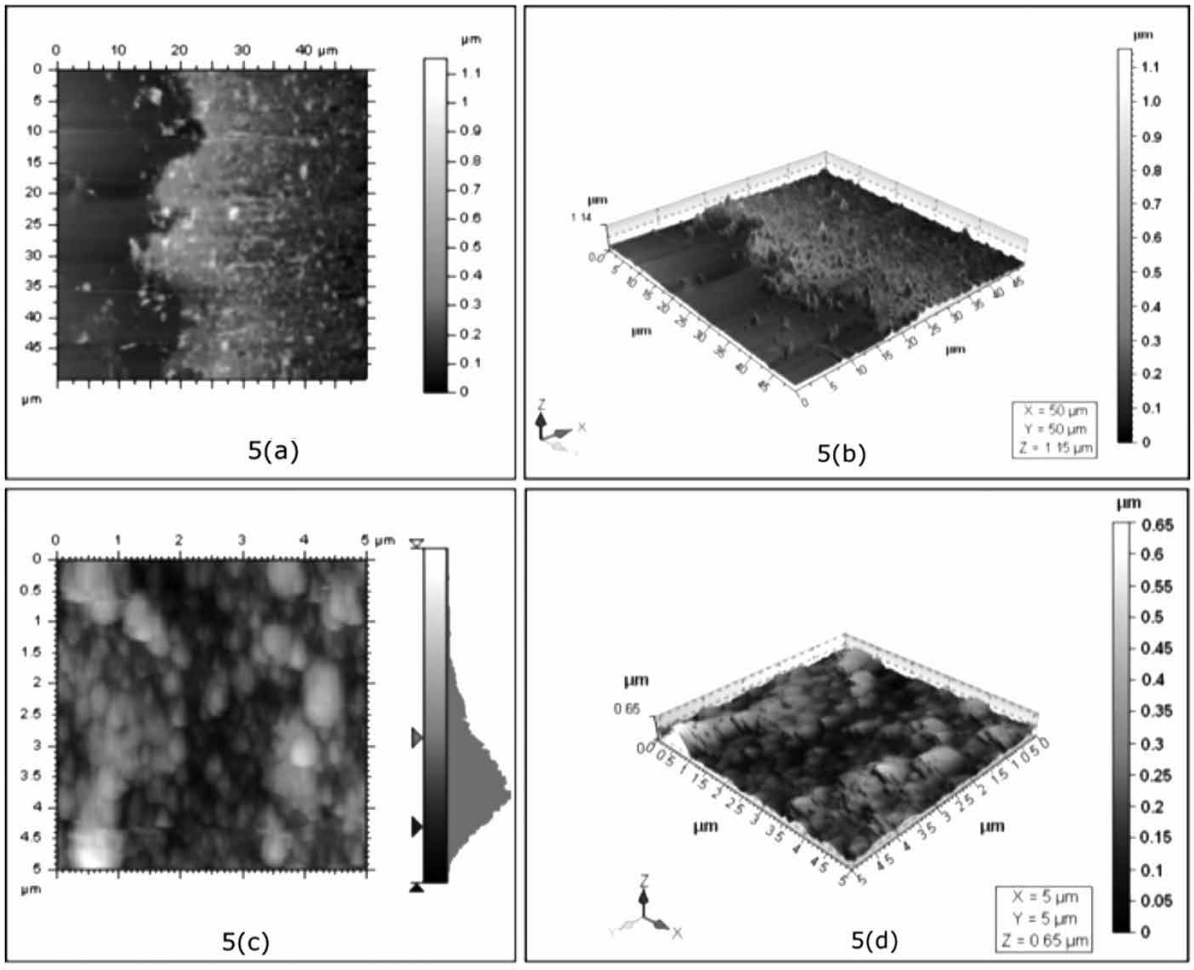

Fig. 5. AFM surface images of ZnO thin films formed on glass substrate with laser exposure (T= 5 min (a) thickness measurement, magnification 50 µm × 50 µm (b) 3-D view of the film (c) roughness measurement of film, and (d) roughness measurement 3-D view

images in Figure 7 correspond to a deposition time of 5 min. The roughness of the films shown in these figures is confirmation of the topography or texture of the surfaces in corresponding cases for AFM microscopy.

The elemental analysis of the thin film using EDS technique showed the presence of zinc and oxygen at 1:1 for 10 minutes on the deposited film. In the case of 5 minutes of deposition, the abundance of oxygen is found to be more than zinc (Table 3).

5.3 Structural investigation of the thin film by XRD

X-ray diffraction technique was used for the structural investigation of ZnO thin films. From the analysis of the XRD pattern of the thin film prepared using PLD, it was confirmed that the thin film exhibited a crystalline nature and seemed to be rough. Different diffraction peaks were identified and the corresponding values of the interplanar lattice parameter, *a* was determined by the relationship,

$$a=(h^2+k^2+l^2)^{1/2}$$

quantities d_{hkl} (h, k, l are Miller Indices) were calculated from the Bragg equation

$$n\lambda = d\ sin\theta$$

and compared with the standard values. The Studies have shown that the ZnO thin film has a polycrystalline hexagonal structure. The Miller indices are also shown in the analysis results in Figures 8 and 9. The polycrystalline hexagonal structure revealed the low island growth model of the thin film. In this model, the film atoms are more tightly bound to each other than to the substrate. In this case 3 dimensional islands nucleate and grow directly on the surface of the thin film.

Table 3. Elemental composition of the thin film recorded after 10 minutes exposure obtained from EDS analysis.

Element	Series	unn. C [wt. - %]	norm. C [wt. - %]	Atom. C [at. - %]
Zinc	K series	33.18	38.94	19.80
Oxygen	K series	52.03	61.06	86.50
Total = 85.2 %				

5.4 Band gap energy determination of ZnO thin film using UV-VIS characterization

Diffuse reflectance measurement of the zinc oxide thin

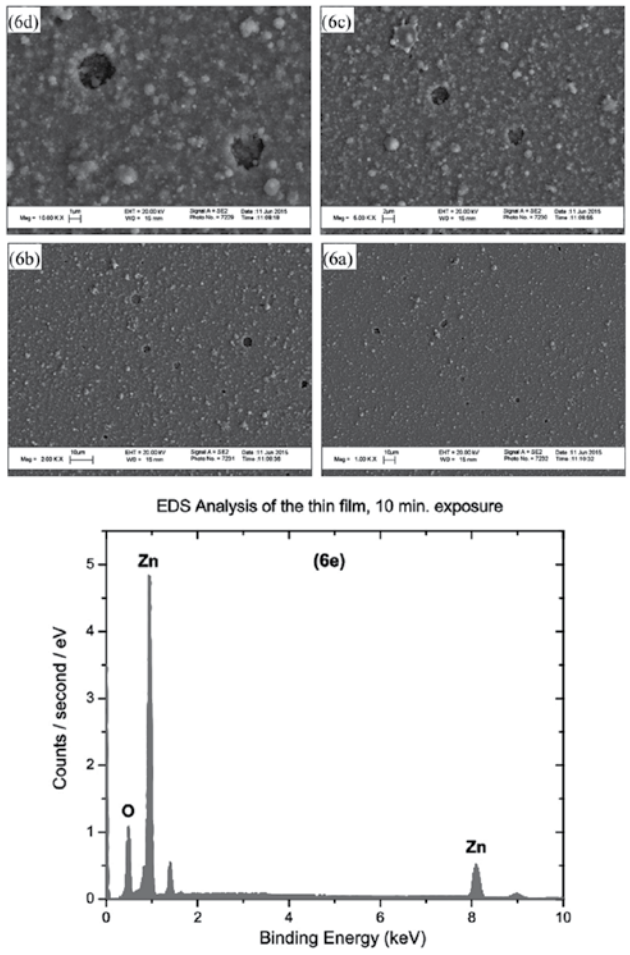

Fig. 6. SEM surface images of ZnO thin film with laser exposure for 10 minutes at various magnifications (a) 10000 × magnification (b) 5000 × magnification (c) 2000 × magnification (d) 1000 × magnification, and (e) EDS analysis of thin film

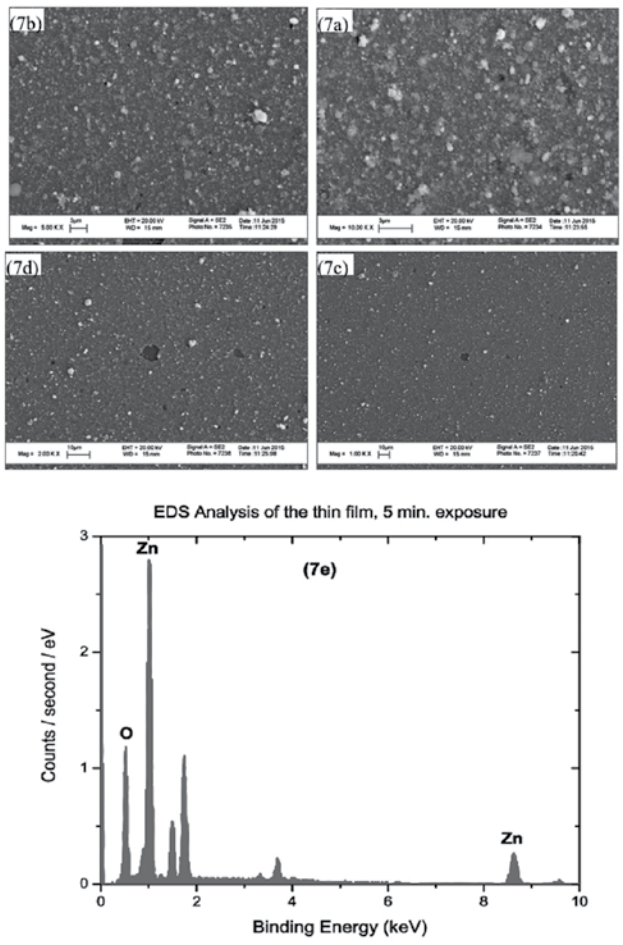

Fig. 7. SEM surface images of ZnO thin film with laser exposure for 5 minutes at various magnifications (a) 10000 × magnification (b) 5000 × magnification (c) 2000 × magnification (d) 1000 × magnification, and (e) EDS analysis of thin film

film was done using UV-VIS spectrophotometer (Shimadzu Model: Solid Spec-3700). The band gap energy of the thin film was determined using the Tauc Plot from the diffuse reflectance spectrum (Adel_*et al.*, 2013), where the Tauc equation is given by

$$(h\upsilon\alpha)^{1/n} = A(h\upsilon - Eg)$$

where h is Planck's constant, υ is the frequency of vibration, α is the absorption coefficient, Eg is the energy band gap, A is the proportional constant, and n denotes the nature of the sample transition.

In the Tauc plot, the x-axis is energy in electron volt which is obtained directly from UV-VIS spectrophotometer. The y-axis is Kubelka-Munk function. Thus, the acquired diffuse reflectance spectrum is to be converted to Kubelka-Munk function (which is obtained directly from the instrument). Thus, the vertical axis is converted into a quantity F (R∞) which is proportional to the absorption coefficient, and the Tauc equation becomes

$$(hvF(R\infty))^2 = A(hv - Eg)$$

Thus, hv is plotted against $(hvF\ (R\infty))^2$. From the plot, a tangent is drawn at the point of inflection and extended towards the x-axis. The x value at the point of intersection is band gap.

The value of band gap energy associated with the hv vs $(hvF\ (R\infty))^2$ curve is the point of intersection of the line tangent on the x-axis. This value is 3.117 and is obtained by extrapolating the tangent passing on the inflection point of the experimental curve. This represents the energy band gap of zinc oxide.

6. Conclusion

PLD film deposition is a robust, economic, and versatile technique. Our homemade vacuum chamber, in which ablation-based films were obtained, allowed for different possibilities for changing physical parameters during the process. Pressure, pulse power, and the number of pulses were changed. Thicker film obtained by femtosecond PLD could be used for a spatial light modulator device. For this purpose, the thicker film with a higher diffraction efficiency is more useful for encoding 3-D interferometric fringes-gratings. Therefore, the formation of

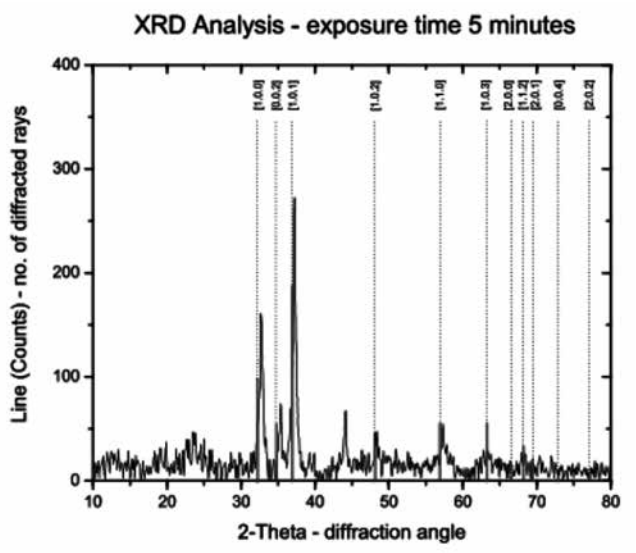

Fig. 8. The XRD analysis result for the thin film with laser exposure time of 5 minutes. The XRD instrument used for the analysis was Siemens D 5000.

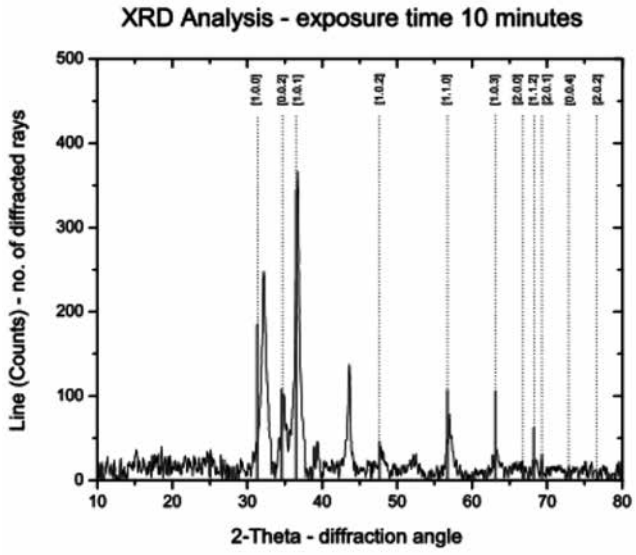

Fig. 9. The XRD analysis result for the thin film with laser exposure time of 10 minutes.

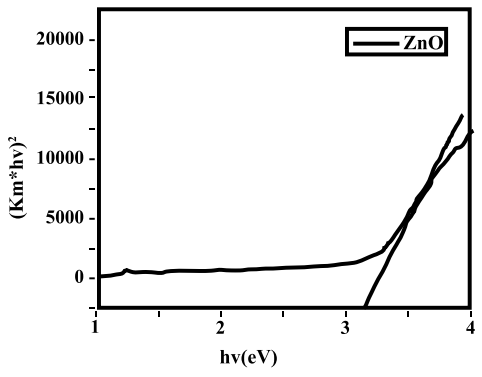

Fig. 10. hν - (hνF (R∞))2 curve for zinc oxide film. Band gap energy, Eg is extracted from x intercept – 2.117 eV. Band gap energy of ZnO is obtained as 3.117 eV.

the film for a process of 5 minutes of laser power and for double the number of pulses or 10 minutes of laser action was studied. AFM, SEM and XRD characterization showed that the uniformity of the deposited film did not decrease when a greater number of pulses was employed. The obtained film can be used for photovoltaic purposes based on the higher width of the band-gap of the quantum well.

ACKNOWLEDGMENTS

We thankfully acknowledge Kuwait University Research Sector general facility projects GS03/01, GS01/08 and the EMU unit in the Faculty of Science, GE01/08 of the Faculty of Engineering at Kuwait University.

References

Taabouche, A., Bouabellou, A., Kermiche, F., Hanini, F., Menakh, S. *et al.* (2013). Effect of substrates on the properties of ZnO thin film grown by Pulsed Laser Deposition. Advances in Materials Physics and Chemistry, **3**: 209-213.

Chrisey, D.B. & Hubler, G.K. (1994). Pulsed Laser Deposition of Thin Films. John Wiley & Sons, Inc., Pp. 55-81

Christen, H.M., Lee, D.F., List, F.A., Cook, S.W., Leonard, K.J. *et.al*. (2005). Pulsed electron deposition of fluorine-based precursors for $YBa_2Cu_3O_{7-x}$-coated conductors. Superconductor Science and Technology, **18**(9): 1168-1175.

Weigand, C.C. (2012). Zinc oxide nanostructures and thin films grown by Pulsed Laser Deposition. Ph.D. thesis, Norwegian University of Science and Technology (NTNU), Trondheim.

Geohegan, D.B. (1994). Diagnostics and characteristics of laser-produced plasmas. In: Chrisey, D.H. & Hubler, G.K. (Ed). Pulsed Laser Deposition of Thin Films. John Wiley & Sons, Inc., New York. Pp.115-162.

Geohegan, D.B. & Puretzky, A.A. (1996). Laser ablation plume thermalization dynamics in background gases: Combined imaging, optical absorption and emission spectroscopy and ion probe measurements. Applied Surface Science, **131**(96-98): 131-138.

Harshavardhan, K.S. & Strikovski, M. (2005). 2nd Generation HTS Conductors, Ed: Goyal, A., Boston, MA: Kluwer-Academic, Pp. 108-133.

Schwarz, H. & Tourtellotte, H.A. (1969). Vacuum deposition by high-energy laser with emphasis on barium titanate films. Journal of Vacuum Science and Technology, **6**(3): 373-378.

Höbel, M., Geerk, J., Linker, G. & Schultheiss, C., (1990). Deposition of superconducting YBaCuO thin films by pseudospark ablation. Applied Physics Letters, **56**(10): 973-975.

Jiang, X.L. & Xu, N. (1989). Preparation of dense films of crystalline ZrO_2 by intense pulsed-electron-beam ablation. Journal of Applied Physics, **66**(11): 5594-5597.

Jahja Kokaj (2011). Characterization of optical and microscopic properties of ZnO film chemically deposited on a glass substrate. Kuwait Journal of Science and Engineering, **38**(2A): 93-106.

Pattar, J., Sawant, S.N. Nagaraja, M., Shashank, N., Balakrishna, K.M., *et.al*. (2009). Structural optical and electrical properties of vacuum evaporated indium doped zinc telluride thin films. International Journal of Electrochemical Science, **4**: 369-376.

Kokaj, J. & Rakhshani, A.E. (2004). Photocurrent spectroscopy of solution-grown CdS films annealed in $CdCl_2$ vapor. Journal of Physics D: Applied Physics, **37**(14): 3727-3737.

Lee, H.N., Christen, H.M., Chisholm, M.F., Rouleau, C.M. & Lowndes, D.H. (2005). Strong polarization enhancement in asymmetric three-component ferroelectric superlattices. Nature, **433**(7024): 395-399.

Lowndes, D.H., Geohegan, D.B., Puretzky, A.A., Norton, D.P. & Rouleau, C.M. (1996). Synthesis of novel thin-film materials by pulsed laser deposition. Science, **273**(5277): 898-903.

Metev, S.M. & Veiko, V.P. (1998). Laser-Assisted Microtechnology. Springer Series in Material Science. Springer-Verlag Berlin Heidelberg, Pp. 228-244

Rakhshani, A.E., Kokaj, J., Mathew, J. & Preadeep, B. (2007). Successive chemical solution deposition of ZnO films on flexible steel substrate: Structure, photoluminescence and optical transitions. Applied Physics A: Materials Science & Processing, **86**(2): 377-383.

Rakhshani, A.E., Bumajdad, A., Kokaj, J. (2007). ZnO films grown by successive chemical solution deposition. Applied Physics A: Materials Science & Processing, **89**(4): 923-928.

Rakhshani, A.E., Bumajdad, A., Kokaj, J. & Thomas, S. (2009). Structure, composition and optical properties of ZnO: Ga films electrodeposited on flexible substrates Applied Physics A: Materials Science & Processing, **97**(4):759-764.

Schölch, H.P., Fickenscher, P., Redel, T., Stetter, M., Saemann-Ischenko, G. *et al.* (1989). Production of $YBa_2Cu_3O_{7-x}$ superconducting thin films by pulsed pseudospark electron beam evaporation. Applied Physics A, **48**(4): 397-400.

Schlom, D.G., Haeni, J.H., Lettieri, J., Theis, C.D., Tian, W., *et al.* (2001). Oxide nano-engineering using MBE. Materials Science and Engineering: B, **87**(3): 282-291.

Sambri, A., Amoruso, S., Wang, X., Radovic, M., Granozio, F.M, Bruzzese R. (2007). Substrate heating influence on plume propagation during pulsed laser deposition of complex oxides. Applied Physics Letters, **91**(15): 151501-1515013.

Smith, H.M. & Turner, A.F. (1965). Vacuum deposited thin films using a ruby laser. Applied Optics, **4**(1): 147-148.

Sivanandan, S.H., Freeman, J.R., Diwakar, J.R. & Hassanein, A. (2014). Femtosecond Laser Ablation: Fundamentals and Applications; Laser-Induced Breakdown Spectroscopy; Springer Series in Optical Sciences,_**182**: 143-166.

Tan, S.T., Chen, B.J., Sun, X.W., & Fan, W.J. (2005). Blueshift of optical band gap in ZnO thin films grown by metal-organic chemical-vapor deposition. Journal of Applied Physics, **98(1)**: 013505-013505-5.

Warusawithana, M.P., Colla, E.V., Eckstein, J.N. & Weissman, M.B. (2003). Artificial dielectric superlattices with broken inversion symmetry. Physical Review Letters, **90**(3): 036802-036806

Willmott, P.R., & Huber, J.R. (2000). Pulsed laser vaporization and deposition. Reviews of Modern Physics, **72**(1): 315-328.

Willmott, P.R. (2004) Deposition of complex multi-elemental thin films. Progress in Surface Science, **76**(6-8): 163-217.

Yamada, H., Kawasaki, M., Ogawa, Y., Tokura, Y. (2002). Perovskite oxide tricolor superlattices with artificially broken inversion symmetry by interface effects. Applied Physics Letters, **81**(25): 4793-4795.

Submission : 10/08/2017
Revision : 19/10/2017
Acceptance : 22/10/2017

ترسيب الجسيمات النانوية المرتكزة على ليزر الفيمتو ثانية على غشاء رقيق وخصائصه

جاهجا كوجاج[1] ، علي شعيب[2]، يعقوب مقدسي[1]، ريميا ناير[1]، جوزيف ماثيو[1]

[1] قسم الفيزياء، كلية العلوم، جامعة الكويت، الكويت
[2] وحدة الهندسة الطبية الحيوية، قسم علم وظائف الأعضاء، كلية الطب، جامعة الكويت

الملخص

يعد ترسيب الجسيمات النانوية المرتكزة على ليزر الفيمتو ثانية تقنية واعدة لتشكيل أغشية رقيقة متجانسة. ونعرض في المقدمة الإطار النظري المتعلق بتقنيات ترسيب الأغشية الرقيقة بما في ذلك ترسيب الليزر النبضي (PLD). ومن ثم نقوم بوصف غرفة محلية الصنع تُستخدم لترسيب الليزر النبضي PLD مع ليزر الفيمتو ثانية. تم استخدام مجهر القوة الذرية (AFM) لقياس خصائص الأغشية الناتجة. تم تصور سمك وخشونة ونسيج سطح الأغشية باستخدام هذه التقنية. تم استخدام تقنيات حيود الأشعة السينية والمسح الالكتروني المجهري لتحديد خصائص طبقة رقيقة من الجسيمات النانوية الناتجة. تم تحديد طاقة فجوة الحزمة لغشاء أكسيد الزنك باستخدام تمايز UV-VIS.